

## Photoproduction of Pion Pairs in Hydrogen\*

MICHEL BLOCH† AND MATTHEW SANDS  
*The California Institute of Technology, Pasadena, California*  
 (Received September 2, 1958)

The photoproduction of pion pairs has been observed by detecting, in a magnetic spectrometer, the negative pions which emerged at 60° and at 120° from a hydrogen target in the bremsstrahlung beam of an electron synchrotron. The yields of negative pions "per equivalent quantum" were measured for several values of the pion energy and the bremsstrahlung cutoff energy. From the variations of the yields with bremsstrahlung cutoff energy, the cross section for the emission of negative pions was obtained. The cross section shows no large dependence on the pion angle from 90° to 150° in the c.m. system. The integral of the cross section over the negative pion energy is consistent with a constant value of about  $4 \times 10^{-30}$  cm<sup>2</sup>/sterad for photon energies between 600 and 1100 Mev. The observed dependence of the cross section on pion energy has been compared to some phenomenological models.

### 1. INTRODUCTION

THE production of pions from the interaction of high-energy quanta with protons has been studied extensively for quantum energies up to 400 Mev. At energies above 400 Mev the photoproduction of pion pairs and higher multiplets becomes energetically possible. The photoproduction of pion pairs was first observed in the 500-Mev bremsstrahlung beam of the Caltech synchrotron by observing the negative pions emitted from a hydrogen target. The conservation of charge requires that at least one other positive light particle is also emitted. The negative pions are presumed to arise from the reaction  $\gamma + p \rightarrow \pi^- + \pi^+ + p$ , or a reaction with three or more pions. The Caltech measurements<sup>1-3</sup> gave evidence for the existence of the process, and showed that the negative pion was most often emitted with a small fraction of the available energy.

More extensive measurements were carried out at Stanford with bremsstrahlung beams up to 600 Mev. Friedman and Crowe<sup>4</sup> measured the yields of negative pions at laboratory angles of 60° and 75° for several pion energies and bremsstrahlung cutoff energies. Their main conclusions were: (a) that the yield of 76-Mev negative pions increased only slowly with energy above the threshold, reaching a value of about  $0.6 \times 10^{-32}$  cm<sup>2</sup>/Mev-sterad (per equivalent quantum) at 600 Mev; and (b) that, at the highest energy, (600 Mev), the energy spectrum of the negative pions was peaked at low energy. Both results are in quantitative agreement with the calculations of Cutkosky and Zachariasen<sup>5</sup> (based on the Chew-Low theory) who concluded that the process should occur predominantly

with the emission of the positive pion in a *P* state and the negative pion in an *S* state. Friedman and Crowe also observed an increase in the yield of positive pions for bremsstrahlung cutoff energies above the pair threshold, which increase they attributed to pions from  $(\pi^+, \pi^-)$  and  $(\pi^+, \pi^0)$  pairs.

Preliminary results have been published of a recent experiment at Cornell<sup>6</sup> where the photoproduction of pion multiplets has been observed in a hydrogen-filled diffusion cloud-chamber. Another group at Cornell<sup>7</sup> has also reported some preliminary results of an experiment similar to that to be described here. The results of these two experiments are compared with ours below. The early results of some of our work have been published.<sup>8</sup>

Information about states which contain a nucleon and two pions has also been obtained from inelastic nucleon-nucleon and pion-nucleon collisions. The results are said to indicate<sup>9-12</sup> the formation and decay of metastable pion-nucleon system which corresponds to the  $T = \frac{3}{2}$ ,  $J = \frac{3}{2}$  resonance in pion scattering.

The intent of the experiment to be described here was to obtain the cross section for the photoproduction of pion pairs for quantum energies up to 1100 Mev from measurements of the negative pions produced in hydrogen. Since the process has three particles in the final state, the knowledge of the energy and the direction of the negative pion is not sufficient to determine the energy of that photon in the bremsstrahlung beam responsible for the reaction. All energies from the threshold to the bremsstrahlung cutoff contribute to the number of pions observed. It was, however, planned to obtain the pion yields with sufficient accuracy at a

\* This work was supported in part by the U. S. Atomic Energy Commission and is based on a thesis submitted by M. B. in partial fulfillment of the requirements for the Ph.D. degree.

† Present address: Ecole Polytechnic, Paris, France.

<sup>1</sup> V. Z. Peterson and I. G. Henry, *Phys. Rev.* **96**, 850 (1954).

<sup>2</sup> Sands, Bloch, Teasdale, and Walker, *Phys. Rev.* **99**, 652 (1955).

<sup>3</sup> V. Z. Peterson, *Bull. Am. Phys. Soc. Ser. II*, **1**, 172 (1956).

<sup>4</sup> R. M. Friedman and K. M. Crowe, *Phys. Rev.* **105**, 1369 (1957).

<sup>5</sup> R. E. Cutkosky and F. Zachariasen, *Phys. Rev.* **103**, 1108 (1958).

<sup>6</sup> Sellen, Cocconi, Cocconi, and Hart, *Phys. Rev.* **110**, 779 (1958).

<sup>7</sup> Woodward, Wilson, and Luckey, *Bull. Am. Phys. Soc. Ser. II*, **2**, 195 (1957).

<sup>8</sup> M. Bloch and M. Sands, *Phys. Rev.* **108**, 1101 (1957).

<sup>9</sup> L. C. L. Yuan and S. J. Lindenbaum, *Phys. Rev.* **103**, 404 (1956).

<sup>10</sup> S. J. Lindenbaum and R. M. Sternheimer, *Phys. Rev.* **105**, 1874 (1957).

<sup>11</sup> R. M. Sternheimer and S. J. Lindenbaum, *Phys. Rev.* **109**, 1723 (1958).

<sup>12</sup> Crew, Hill, and Lavatelli, *Phys. Rev.* **106**, 1051 (1957).

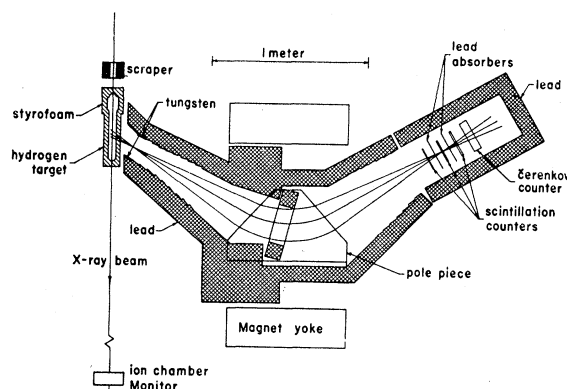


FIG. 1. Diagram of the experimental arrangement. The diagram is a cross section through a horizontal plane of symmetry.

few bremsstrahlung cutoff energies so that differences in the pion yields for successive cutoff energies could be used to obtain the cross section for photons of a particular energy.

## 2. THE EXPERIMENT

A diagram of the experimental arrangement is given in Fig. 1. Negative pions produced in the hydrogen target by the x-ray beam were analyzed for momentum by the magnetic spectrometer, traversed a set of counters, and were counted electronically.

### The Target and X-Ray Beam

The target consisted of a cylindrical vessel (with hemispherical ends) 43 cm long and 5 cm in diameter with a 0.075-cm-thick steel wall, surrounded by a 4-cm layer of Styrofoam insulation. The vessel was cooled, by thermal contact to a liquid nitrogen reservoir, to a mean temperature of about 100°K as measured by thermocouples in contact with the walls at two points. Hydrogen gas held in the target at a pressure of 150 atmospheres (measured with a calibrated Bourdon gauge) was assumed to be in thermal equilibrium with the target wall. The hydrogen density, determined from the measurements of pressure and density using the data of Johnston *et al.*,<sup>13</sup> was about 0.03 g/cm<sup>3</sup>. The error in the determination of the gas density was about 3%, but the relative error in the density measurement for different runs is estimated to be about 1%.

The x-ray beam was collimated at the synchrotron so that its diameter at the target (about 4 cm) was slightly less than the inner diameter of the target wall. A lead "scraper" immediately in front of the target prevented radiation scattered at the primary collimator from striking the target wall, but did not intercept any of the primary beam. After the target, the x-ray beam traversed the collimators and target of another experiment and entered a monitoring ionization chamber.

<sup>13</sup> H. L. Johnston *et al.*, U. S. Atomic Energy Commission Report MDDC-850 (unpublished).

The charge collected from the chamber was recorded by an integrating electrometer, and at each synchrotron energy is proportional to the energy flux in the beam. Due in part to the collimation after our experiment and in part to characteristics of the chamber, the proportionality constant varied somewhat with the synchrotron energy. The relation between the flux through the hydrogen target and the integrator readings was determined as a function of synchrotron energy by measurements with an ionization chamber placed directly behind the target, which chamber was in turn calibrated against a "quantometer" constructed according to the design of Wilson.<sup>14</sup> During this experiment the synchrotron was generally operating with an x-ray flux through the collimators of about  $10^{11}$  Mev per pulse at one pulse per second.

The synchrotron was operated so that the electrons struck the internal radiator at a more or less constant rate during a 20-millisecond interval over which the magnetic field in the synchrotron was held constant to about 0.1%. The energy of the electrons which struck the target in this interval was determined from a continual measurement of the magnetic field at the "plateau" of the field. The energy measurement had an uncertainty of a few percent due to the unknown details of the orbit shape, but was reproducible to 0.1%, and had about this accuracy for relative measurements at nearby energies. The energy measurements for each run were used to obtain an average energy for each set of experimental data.

### The Magnet

Particles emitted from the hydrogen in a small angular interval were analyzed by a uniform-field magnetic spectrometer. The particles accepted by the magnet were restricted by a lead aperture 25 cm wide, about 6.5 cm high, and about 10 cm thick (in the direction along the trajectories) placed within the 10-cm gap between the magnet poles in such a way as to eliminate particles scattered from the pole surfaces. This aperture, located at about 120 cm from the target determined the solid angle of acceptance, 0.020 sterad, of the spectrometer. An aperture of tungsten and lead placed near the target restricted the origin of the particles detected to a region between the ends of the target (thus excluding the particles produced in the steel ends). The dispersion of the spectrometer was such that particles accepted by the counters had momenta in an interval whose width was 16% of the central momentum. The central momentum was adjustable to a maximum of 255 Mev/*c* at a field of 1.4 webers/m<sup>2</sup> (corresponding to a pion energy of 150 Mev). The spectrometer was shielded from stray radiation by 10 cm or more of lead on all sides in the plane of the x-ray beam.

The diagram of Fig. 1 shows the arrangement of the

<sup>14</sup> R. R. Wilson, Nuclear Instr. 1, 101 (1957).

magnet and counters for the measurements at  $60^\circ$ . For the measurements at  $120^\circ$  the same geometry, reflected about a line perpendicular to the x-ray beam at the target, was used.

### The Counters

The counter system consisted of three scintillation counters and a Čerenkov counter. Each scintillation counter consisted of a thin rectangle of scintillation plastic joined by Lucite light pipes, at the two smaller edges, to two photomultiplier tubes whose outputs were connected in parallel. The first two counters were 15 cm wide and determined the momentum acceptance interval. The third counter was 18 cm wide and intercepted all particles which traversed the first two. The heights of the counters (23 cm, 23 cm, and 25 cm, respectively) were such as to include all particles from the target which traversed the magnet. The thickness of the counters was 0.69, 1.27, and 1.27 cm, respectively, and was sufficient to give a well-defined "peak" in the pulse spectrum from minimum ionizing particles. The spread of pulse amplitudes for minimum particles was about 30 to 40%.

Lead absorbers about 0.6 cm thick were placed directly after the first and after the second scintillation counters. These had little influence on the pions traversing the counters, but served to remove a large background of spurious coincidences due, apparently, to soft electromagnetic radiation which penetrated the shielding.

The particles accepted by the spectrometer consisted of electrons, pions and protons (the latter only on positive-particle runs). Protons of the maximum selected momentum did not have a range sufficient to penetrate to the third scintillation counter. Since the resolution of the scintillation counters did not, in general, permit the separation of pions and electrons on the basis of their energy loss, a Čerenkov counter was designed which had a large difference in its sensitivity to the two particles.

The Čerenkov counter was a rectangular block of Lucite 20 cm by 28 cm by 5 cm. It was viewed by two photomultipliers in contact with the centers of the smaller edges. The large faces were covered with black paper *not* in close contact with the surface so that the Čerenkov light, emitted by particles moving nearly perpendicular to the large face, could reach the photomultipliers only by several internal reflections. Thus, although the threshold for Čerenkov emission is at  $\beta=0.67$ , the threshold for internal reflection is, for particles moving normal to the surface, at  $\beta=0.9$ . Since pions of the maximum energy detected (150 Mev) have a  $\beta=0.88$ , whereas electrons of the same momentum have  $\beta\approx 1$ , it was expected that the two would give widely different responses. This expectation is confirmed by the measurements described below.

The pulses from the counters were amplified and

shaped to a duration of  $0.3 \mu\text{sec}$  and fed to a coincidence circuit which was biased to operate on pulses well below the pulse distributions from the scintillation counters, and for the Čerenkov counter at a bias which gave nearly maximum efficiency for electrons. The coincidence circuit registered events which gave pulses in all three scintillation counters within the resolving time of  $0.25 \mu\text{sec}$ , and also those events *not* accompanied by a pulse from the Čerenkov counter within the anticoincidence resolution of  $0.5 \mu\text{sec}$ . The anticoincidence signal was also used to trigger an 8-channel pulse-height analyzer with which it was possible to check periodically the pulse distributions from the scintillation counters. The coincidence circuit also registered events in which the first two counters were in coincidence with pulses which occurred  $1 \mu\text{sec}$  later in the third counter. The rate of these events was used to compute corrections for accidental coincidences.

### The Measurements

The counting rates for 3-fold coincidences with and without a coincident pulse in the Čerenkov counter were measured at  $60^\circ$  and at  $120^\circ$ , with the spectrometer set for pions of energy 50, 100, and 150 Mev, and for synchrotron energies of about 600, 700, 900, and 1100 Mev. Background runs were made for each setting with the target containing one atmosphere of hydrogen at room temperature, corresponding to a gas density  $1/400$  that present in the "full-target" runs. The background rates, which were 10% or less, were subtracted from the full-target counting rates. A correction for accidental coincidences, which amounted to about 2%, was made to the 3-fold rates. The accidental rate for 4-fold coincidences was negligible.

Due to the large size of the counters, the counting rate of cosmic rays was significant. The number of cosmic rays counted was minimized by gating the counting circuits so that they were sensitive only during the spill-out time of the x-ray beam. The cosmic-ray rate was then small, but not negligible. To correct for it, the cosmic-ray rate was measured, and the total sensitive time of each run was obtained by counting, also in the gated counters, pulses from a fixed-frequency oscillator. From these quantities the cosmic-ray contribution to each set of data could be computed. It amounted, typically, to about 5%.

From the corrected 3-fold and 4-fold coincidences, and a knowledge of the efficiency of the Čerenkov counter for pions and for electrons, the number of pions which traversed the counters can be obtained. Let  $N_3$  be the number of 3-fold coincidences *not* accompanied by a Čerenkov pulse, and  $N_4$  be the number of 4-fold coincidences in a particular run. (We choose to work with these two quantities because they are statistically independent so that their errors can be combined in the usual way.) If  $\mathcal{E}_e$  and  $\mathcal{E}_\pi$  are the efficiencies of the Čerenkov counter for electrons and

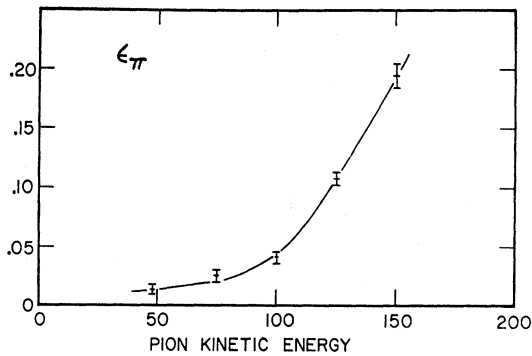


FIG. 2. The efficiency  $\epsilon_\pi$  of the Čerenkov counter for pions as a function of the pion kinetic energy.

pions, respectively, then the number of pions counted is

$$n_\pi = \frac{\epsilon_e}{\epsilon_e - \epsilon_\pi} \left[ n_3 - \left( \frac{1 - \epsilon_e}{\epsilon_e} \right) n_4 \right]. \quad (1)$$

One would, obviously, like  $\epsilon_\pi$  to be small and  $\epsilon_e$  to be near one.

The efficiencies  $\epsilon_e$  and  $\epsilon_\pi$  were determined by some auxiliary measurements. The efficiency for electrons was obtained by setting the magnet to accept particles at  $35^\circ$  with a momentum of 100 Mev/c, and by replacing the hydrogen target with a thin lead target to obtain a large flux of electrons through the spectrometer. Pions of the selected momentum would not penetrate into the third counter and were, therefore, not counted. The electron efficiency obtained in this way was  $0.70 \pm 0.02$ . Runs at higher momenta gave the same value supporting the belief that the electron efficiency should be independent of electron energy and that the ratio of pions to electrons from the lead was small. The sources of inefficiency were investigated and found to be in part (about  $\frac{1}{3}$ ) due to electrons lost by scattering or interaction in the thin lead absorbers between the counters, and for the rest, due to the failure of relativistic particles to give a pulse above the counting bias of the Čerenkov counter. (Since the average number of photoelectrons produced in the Čerenkov light was only about 10 or so the spread in pulse heights was large.) The electron efficiency is sufficiently large in comparison with the pion efficiency as to give a fairly clear separation between the two types of particles.

The efficiency of the Čerenkov counter for pions was determined by counting the relatively pure flux of *positive* pions from the hydrogen target with the magnet at  $60^\circ$  and with the momentum set for pions from the photoproduction resonance. A correction for the small electron contamination was made by subtracting from the positive-pion run the counts observed in an equal run with the magnetic field reversed. With the field set for negative particles the pion rate is much lower, but the electron rate is presumed to be the same. The difference corresponds, therefore, to a pure beam

of pions. The efficiency obtained for several pion energies is shown in Fig. 2. The efficiency of the Čerenkov counter for pions was checked at periodic intervals during the experiment and no significant change was observed.

The 3-fold coincidences observed in all the measurements were found to be predominantly due to pions, the electron rates varying from 0.1 to 0.3 of the pion rates. The source of these electrons was not investigated. The errors in the pion rates are, therefore, due primarily to the statistical error in the observed 3-fold coincidences, the assigned errors of 0.02 in  $\epsilon_e$  and 0.01 in  $\epsilon_\pi$  adding only a little to the total assigned errors.

A small correction was made to the number of pions counted for negative pions produced singly on impurities in the hydrogen. An analysis<sup>15</sup> of the hydrogen used in the target showed a relative molar concentration of oxygen and nitrogen of  $6 \times 10^{-4}$  and  $4 \times 10^{-4}$ , respectively. From the data of Littauer and Walker<sup>16</sup> on the negative to positive ratio from carbon and oxygen, and the known single-pion rate from hydrogen, an estimate was made of the negative pions produced in the impurities. The correction amounted to about 3% of the pion rates at highest synchrotron energy.

We considered the possibility that negative pions produced in the steel end of the target could be scattered by the hydrogen into the counting aperture, and that photons from neutral pions produced in the hydrogen could produce negative pions in the target walls. An estimate of these second-order effects shows them to be completely negligible.

### 3. RESULTS

#### Pion Yields

The pion rates  $R_-$ , defined as the number of negative pions produced in hydrogen and registered by the counters, per unit energy of the x-ray beam, were obtained from the corrected number of pions and the energy flux as measured by the monitoring ionization chamber. We define  $\sigma(T, \theta, k)$  as the cross section for the production in hydrogen, by a photon of energy  $k$ , of a negative pion of energy  $T$  at the angle  $\theta$ , per unit energy interval (in  $T$ ) and per unit solid angle. This cross section is related to  $R_-$  by

$$R_- = \eta_- C \Delta \Omega \Delta T \int_0^{E_0} \sigma(T, \theta, k) N(E_0, k) dk, \quad (2)$$

where  $C$  is the number of hydrogen atoms per unit area in the effective length of the target;  $\Delta \Omega$  is the solid angle of acceptance of the magnet;  $\Delta T$  is the energy spread of the pions which intercept the counters;  $N(E_0, k) dk$  represents the number of photons of energy between  $k$  and  $k + dk$  which traverse the target per

<sup>15</sup> The analysis was done with a mass spectrometer by the Consolidated Electroynamics Corporation.

<sup>16</sup> R. M. Littauer and D. Walker, Phys. Rev. **86**, 838 (1952).

unit energy of the beam, for a bremsstrahlung cutoff energy  $E_0$ ; and  $\eta_-$  is correction factor for those pions which are not counted due to decay in flight or through absorption in the counter system.

For reactions in which it is not possible to infer the relevant photon energy from the kinetics of the observed particle, it is usual to express the observations in terms of a "yield per equivalent quantum" which has the dimensions of a cross section and is defined as

$$\sigma^*(T, \theta, E_0) = E_0 \int_0^{E_0} \sigma(T, \theta, k) N(E_0, k) dk. \quad (3)$$

The yield per equivalent quantum is then given in terms of the pion rate by

$$\sigma^*(T, \theta, k) = E_0 R_- / (\eta_- C \Delta \Omega \Delta T). \quad (4)$$

The instrumental coefficient  $[\eta_- C \Delta \Omega \Delta T]$  can be computed from the known instrumental parameters. The decay-correction,  $\eta_-$ , involves, however, a laborious computation to determine the number of decay muons which enter the counters. To avoid this computation and other corrections (such as slit penetration) the experimental parameters were determined in terms of the known cross section for the single production of positive pions by reversing the magnetic field and counting positive pions with the synchrotron operating at 490 Mev. This measurement was made for 125-Mev pions at  $60^\circ$ , which corresponds to the resonance in single production. No pions from pair processes are counted under these conditions. The observed positive-pion counting rate  $R_+$  is related to the known cross section by

$$R_+ = [\eta_+ C \Delta \Omega \Delta T] N(E_0, k_0) \sigma_+(\theta, k_0) (\partial k_0 / \partial T), \quad (5)$$

where  $\sigma_+(\theta, k_0)$  is the differential cross section for positive-pion production in hydrogen at the photon energy  $k_0$  defined by the angle and energy of the pion, and  $\partial k_0 / \partial T$  is the rate of change of  $k_0$  with  $T$ , holding  $\theta$  constant. All quantities outside the brackets are known:  $N(E_0, k_0)$  from the photon spectrum (see below) and  $\sigma_+(\theta, k_0) = (21.3 \pm 2.0) \times 10^{-30}$  cm<sup>2</sup>/sterad for  $\theta = 60^\circ$  and  $k_0 = 300$  Mev from the data of Walker *et al.*<sup>17</sup> The bracketed quantity is, therefore, determined from the measurement of  $R_+$ .

From the quantity within the brackets in Eq. (5) we have determined the corresponding quantity which appears in Eq. (4) in the following way:  $C$  and  $\Delta \Omega$  are taken to be independent of the energy and charge of the pion and the energy dependence of  $\Delta T$  is assumed to be given by the constant relative momentum acceptance ( $\Delta p / p$ ) of the magnet. The decay correction  $\eta$  consists of two parts<sup>18</sup>: a factor for those pions which decay in flight before reaching the counters; and a

<sup>17</sup> Walker, Teasdale, Peterson, and Vette, Phys. Rev. **99**, 201 (1955).

<sup>18</sup> The details of the decay correction have been described in reference 17.

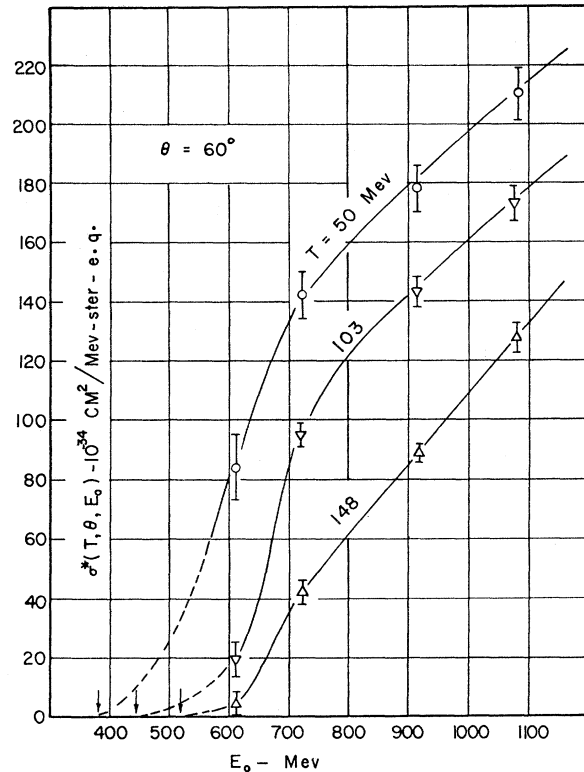


FIG. 3. The negative-pion yields at  $60^\circ$ . The ordinate is the yield from hydrogen of negative pions of kinetic energy  $T$  for a bremsstrahlung cutoff energy  $E_0$ . The yield is expressed as a cross section per equivalent quantum, and per unit energy and solid angle of the pion.

term which takes into account those decay muons which traverse the counters. The decay factor, which corresponds to a pion loss of about 20%, has a simple energy dependence. The muon term depends in a complicated way on the whole spectrum of pions which enter the aperture of the apparatus, and acts to reduce the decay correction to about 10%. The energy dependence of this term has been estimated. We believe that uncertainties in the decay correction will contribute not more than 2% to the errors of the computed pion yields.

The over-all uncertainty in the magnitude of the coefficient  $[\eta_- C \Delta \Omega \Delta T]$  is about 10% and is due mainly to the error in the positive-pion cross section used in the calibration. This systematic error applies to all the results given below, where, however, only the statistical errors of this experiment are given.

The yields per equivalent quantum obtained in this experiment are given in Figs. 3 and 4 as a function of the bremsstrahlung cutoff energy  $E_0$  for the several laboratory energies and angles of the negative pion. The errors shown are standard deviations due mainly to the statistical error in the counting of the negative pions, but with a small contribution from the uncertainty in the efficiency of the Čerenkov counter.

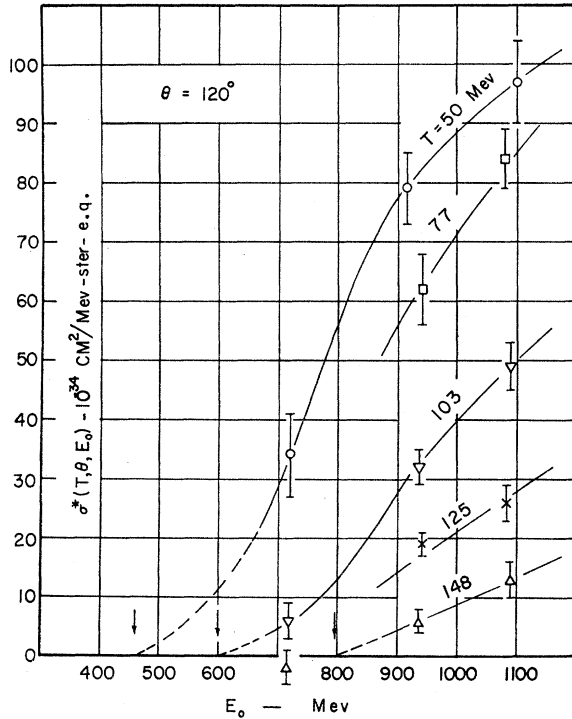


FIG. 4. The negative-pion yields at  $120^\circ$ . The ordinate is the same as in Fig. 3.

The broken line parts of the curves are smooth extrapolations to the kinematic thresholds for the two-pion process, which are indicated by the arrows along the axis of abscissas.

The yields of Figs. 3 and 4 can be compared with some earlier experimental results. The yield of about  $50 \times 10^{-34}$   $\text{cm}^2/\text{Mev steradian}$  (for  $\sigma^*$ ) reported by Friedman and Crowe<sup>4</sup> for 76-Mev negative pions at  $60^\circ$  and a 600-Mev bremsstrahlung beam agrees with an interpolation of our results at 610 Mev. The preliminary results of Woodward *et al.*<sup>6</sup> for measurements of 40-Mev pions at  $35^\circ$  for values of  $E_0$  up to 850 Mev show about twice the yields we observe for 50 Mev pions at  $60^\circ$ ; a result which is consistent with the angular trends that we observe.

### Cross Sections

The cross section  $\sigma(T, \theta, k)$  for the production of negative pions by photons of energy  $k$  can be obtained from the yields given above and a knowledge of the energy spectrum of photons in the x-ray beam. Following the usual practice, we set

$$N(E_0, k) = (1/kE_0)B(E_0, k), \quad (6)$$

where  $B(E_0, k)$  is then  $\approx 1$  and can usually be taken as a function of  $k/E_0$  only. Walker and co-workers,<sup>19</sup> using a pair-spectrometer, have measured the spectrum

<sup>19</sup> Donoho, Emery, and Walker (private communication).

of photons from the tantalum radiator of the Caltech synchrotron. They find that the spectrum agrees with the theoretical "thin-target" spectrum<sup>20</sup> for the lower photon energies ( $k \leq 0.7E_0$ ), but that at the higher energies the function  $B(E_0, k)$  shows neither the gradual rise with increasing  $k$  nor the smooth drop for  $k$  near  $E_0$  which is given by the theory.

In Fig. 5 we show  $B(E_0, k)$  computed for a thin tantalum radiator with  $E_0 = 750$  Mev (solid curve). The measured spectrum is in accord with this curve for low values of  $k$ , but is consistent with the constant value of 0.90 shown by the broken line for large  $k$ . We adopt this experimental curve for the interpretation of our results, and take it to be the same function of  $k/E_0$  for all  $E_0$  from 500 to 1100 Mev. The spectrum we have adopted can be expressed algebraically by

$$B(E_0, k) = \begin{cases} (27/20)(1 - k/E_0 + \frac{3}{4}k^2/E_0^2); & 0 < k < \frac{2}{3}E_0 \\ = 9/10; & \frac{2}{3}E_0 < k < E_0 \\ = 0; & E_0 < k. \end{cases} \quad (7)$$

In terms of  $B(E_0, k)$ , Eq. (3) becomes

$$\sigma^*(T, \theta, E_0) = \int_0^{E_0} \sigma(T, \theta, k) B(E_0, k) dk/k. \quad (8)$$

The increase in the yield  $\sigma^*(T, \theta, E_0)$  with increasing synchrotron energy  $E_0$  is due primarily—but not exclusively—to the cross section for the photons at the high-energy end of the spectrum. The small contribution of the lower-energy photons is easily taken into account by solving Eq. (8) for  $\sigma(T, \theta, k)$  by standard methods. The solution can be expressed as a series which is rapidly convergent for the particular functions encountered here. For our purpose we need retain only

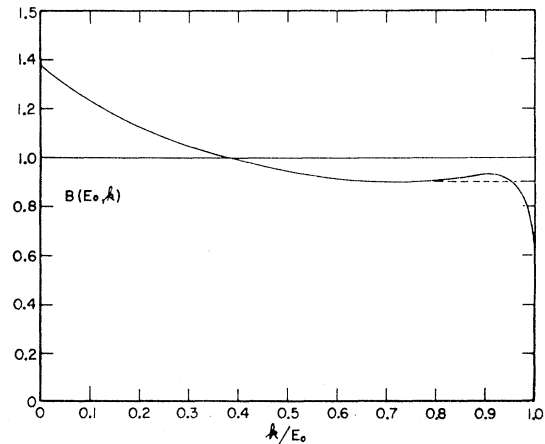


FIG. 5. The bremsstrahlung spectrum function.  $(E_0/k)B(E_0, k)$  gives the number of photons per unit energy interval at  $k$  for a unit energy of flux in the x-ray beam produced by electrons of energy  $E_0$ . The solid curve is the theoretical "thin target" spectrum (given by quantum electrodynamics). The dashed curve is a fit to the measured spectrum for  $(k/E_0) > \frac{2}{3}$ .

<sup>20</sup> H. A. Bethe and W. Heitler, Proc. Roy. Soc. (London) **A146**, 83 (1934).

the first two terms. We have, then,

$$\sigma(k = E_0)$$

$$= \frac{E_0}{B_0} \left[ \frac{d\sigma^*(E_0)}{dE_0} + \frac{1}{B_0} \int_0^{E_0} \frac{\partial^2 B(E_0, E_0')}{\partial E_0' \partial E_0} \sigma^*(E_0') dE_0' \right], \quad (9)$$

where  $B_0$  is given by

$$B_0 = \lim_{k \rightarrow E_0} B(E_0, k) = 0.9, \quad (10)$$

and where we have suppressed temporarily the explicit dependences on  $T$  and  $\theta$  which appear identically in both  $\sigma$  and  $\sigma^*$ .

The first term of Eq. (9) has been evaluated from the data for each adjacent pair of values of  $E_0$  by taking

$$\frac{d\sigma^*(E_0)}{dE_0} = \frac{\sigma^*(E_2) - \sigma^*(E_1)}{E_2 - E_1}, \quad (11)$$

and taking for the relevant photon energy

$$k = \frac{1}{2}(E_2 - E_1). \quad (12)$$

The average cross sections from the threshold to the first energy at which measurements were taken were also obtained by setting  $E_1$  equal to the kinematic threshold and taking  $\sigma^*(E_1) = 0$ .

The integral in Eq. (9) is a small correction to the first term. It has been evaluated by a numerical integration taking  $B(E_0, k)$  as given by Eq. (7) and using the curves of Figs. 3 and 4 for  $\sigma^*$ . The integral was negligible in most cases and amounted to about 10% in the largest case. Since the integral was comparable to, or less than, the statistical error in the

TABLE I. The differential cross section  $\sigma(T, \theta, k)$  for the production in hydrogen of negative pions of kinetic energy  $T$  at the angle  $\theta$  in the laboratory (per unit energy and solid angle) by photons of energy  $k$ . The cross sections are averages over an interval  $\Delta k$  centered at  $k$ , and are given in units of  $10^{-32} \text{cm}^2/\text{Mev-sterad}$ .

| $T$<br>(Mev) | $k$<br>(Mev) | $\theta = 60^\circ$ |                        | $\theta = 120^\circ$ |                        |         |
|--------------|--------------|---------------------|------------------------|----------------------|------------------------|---------|
|              |              | $\Delta k$<br>(Mev) | $\sigma(T, \theta, k)$ | $\Delta k$<br>(Mev)  | $\sigma(T, \theta, k)$ |         |
| 50           | 500          | 220                 | 2.2±0.3                |                      |                        |         |
|              | 670          | 110                 | 3.8±1.0                | 610                  | 220                    | 1.0±0.2 |
|              | 820          | 190                 | 1.7±0.5                | 830                  | 210                    | 1.9±0.4 |
|              | 1000         | 170                 | 1.9±0.7                | 1020                 | 160                    | 1.2±0.7 |
| 77           |              |                     |                        | 750                  | 400                    | 1.3±0.1 |
|              |              |                     |                        | 1010                 | 140                    | 1.8±0.7 |
| 103          | 540          | 140                 | 0.8±0.4                |                      |                        |         |
|              | 670          | 110                 | 5.1±0.5                | 660                  | 120                    | 0.4±0.2 |
|              | 820          | 200                 | 2.2±0.3                | 830                  | 220                    | 1.1±0.2 |
|              | 1000         | 160                 | 2.0±0.5                | 1010                 | 150                    | 1.3±0.4 |
| 125          |              |                     |                        | 810                  | 260                    | 0.7±0.1 |
|              |              |                     |                        | 1010                 | 140                    | 0.6±0.1 |
| 148          | 580          | 70                  | 0.4±0.5                |                      |                        |         |
|              | 670          | 110                 | 2.6±0.5                |                      |                        |         |
|              | 820          | 200                 | 2.2±0.3                | 860                  | 160                    | 0.4±0.2 |
|              | 1000         | 160                 | 2.7±0.4                | 1010                 | 150                    | 0.5±0.3 |

TABLE II. The differential cross section  $\sigma'(T', \theta', k)$  in the c.m. system for the photoproduction of negative pions in hydrogen. The c.m. pion energy and angle are  $T'$  and  $\theta'$ , and  $k$  is the laboratory photon energy.

| $k$<br>(Mev) | $T'$<br>(Mev) | $\theta'$ | $\sigma'(T', \theta', k)$<br>( $10^{-32} \text{cm}^2/\text{Mev-sterad}$ ) |
|--------------|---------------|-----------|---|
| 500          | 35            | 91°       | 1.9±0.3   |
| 540          | 79            | 86°       | 0.7±0.4   |
| 580          | 118           | 85°       | 0.3±0.4   |
| 610          | 103           | 144°      | 1.5±0.3   |
| 670          | 38            | 98°       | 3.4±0.8   |
| 670          | 80            | 90°       | 4.4±0.5   |
| 670          | 118           | 88°       | 2.2±0.4   |
| 660          | 170           | 142°      | 0.5±0.3   |
| 820          | 40            | 104°      | 1.5±0.4   |
| 820          | 81            | 95°       | 1.9±0.3   |
| 820          | 118           | 92°       | 1.9±0.2   |
| 830          | 110           | 147°      | 3.1±0.7   |
| 750          | 138           | 144°      | 2.0±0.2   |
| 830          | 187           | 144°      | 1.7±0.3   |
| 810          | 220           | 143°      | 0.9±0.1   |
| 860          | 256           | 144°      | 0.5±0.3   |
| 1000         | 42            | 110°      | 1.8±0.6   |
| 1000         | 83            | 100°      | 1.8±0.4   |
| 1000         | 119           | 97°       | 2.3±0.4   |
| 1020         | 121           | 150°      | 2.1±1.2   |
| 1010         | 162           | 148°      | 2.9±1.2   |
| 1010         | 203           | 147°      | 2.0±0.6   |
| 1010         | 240           | 146°      | 0.9±0.5   |
| 1010         | 274           | 146°      | 0.8±0.5   |

dominant term, no error has been assigned to the integral.

The cross sections obtained by the above procedure are given in Table I. In the table the interval  $\Delta k$  over which the average cross section has been obtained is just the difference ( $E_2 - E_1$ ) of the two cutoff energies used for determining  $\sigma$ . The errors given for the cross sections are due exclusively to counting statistics, all other random errors being negligible compared with these. Of course the systematic uncertainty of about 10% in the absolute value of the yields applies also to the cross sections.

### c.m. Cross Sections

It is convenient to refer the cross sections to the center-of-momentum (c.m.) system of the incoming quantum and the proton. If  $\sigma'(T', \theta', k)$  is the cross section for the production of a negative pion with kinetic energy  $T'$  and angle  $\theta'$  in the c.m. system (per unit energy and solid angle of the negative pion), then

$$\sigma'(T', \theta', k) = (\hat{p}'/\hat{p})\sigma(T, \theta, k), \quad (13)$$

where  $\hat{p}$  and  $\hat{p}'$  are the momenta of the pion in the laboratory and c.m. systems, respectively. For each entry of Table I we have computed the corresponding energies and angles in the c.m. system and the c.m. cross section. The results are given in Table II where

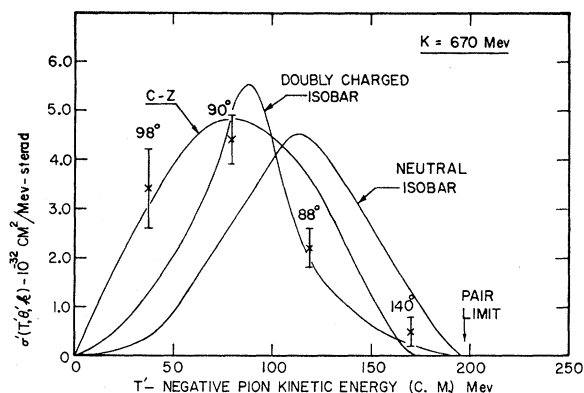


FIG. 6. The c.m. cross section for 670-Mev photons as a function of the pion kinetic energy (c.m.). The c.m. angle of the negative pion is given for each point.

we have grouped together the data which correspond to approximately the same photon energy.

The cross sections of Tables I and II fall into two groups, one for c.m. angles near  $95^\circ$  and the other for angles near  $145^\circ$ . The data for the smaller angle correspond to lower c.m. energies than those for the larger angle. The data for the two angles taken together cover the full range of possible energies for the negative pions from the pair production process. In Fig. 6 we have plotted all the data for photon energies near 670 Mev. The angle of emission of the pion in the c.m. system is given above each plotted point. The energetic upper limit for pions from pairs produced by 670-Mev photons is shown by the arrow. Figures 7 and 8 are corresponding plots for photon energies of 830 and 1010 Mev. The curves in the figures will be discussed below.

In the plots for 830 and 1010 Mev the data for angles near  $95^\circ$  join smoothly with those for angles near  $145^\circ$ . We conclude that there is no large angular dependence of the cross section between these two angles, and that we can tentatively assume that the combined data give the energy spectrum of the negative pions from the pair process at these angles.

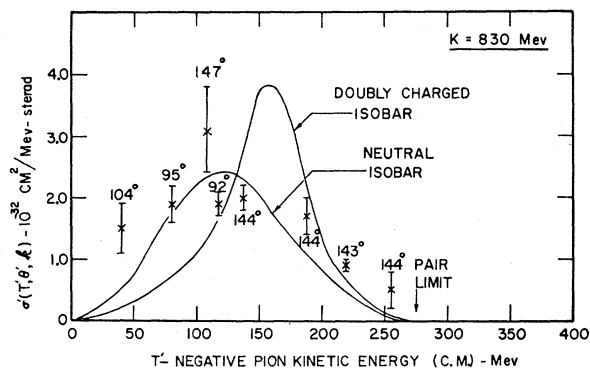


FIG. 7. The c.m. cross section for 830-Mev photons as a function of the pion kinetic energy (c.m.). The c.m. angle of the negative pion is given for each point.

### Integrated Cross Sections

A cross section per unit solid angle  $\sigma'(\theta', k)$  can be obtained by integrating the cross sections of Figs. 6, 7, and 8 over energy. To obtain the integrals we have taken the area under a smooth curve which passes through the data and falls to zero at zero energy and at the maximum allowed energy. These cross sections are given in Table III. If we assume further that the negative pions are emitted with complete angular isotropy in the c.m. system, we can obtain a total cross section by taking  $\sigma_i(k) = 4\pi\sigma'(\theta', k)$ . These total cross sections are also given in Table III. The cross sections of Table III are probably uncertain to about 25%. Within this uncertainty it appears that the cross section is independent of photon energy from about 600 to 1100 Mev. The cross section obtained here agrees with the value of about 60 microbarns obtained recently by Sellen *et al.*<sup>6</sup> using a hydrogen diffusion chamber. These authors find very little triple meson production;

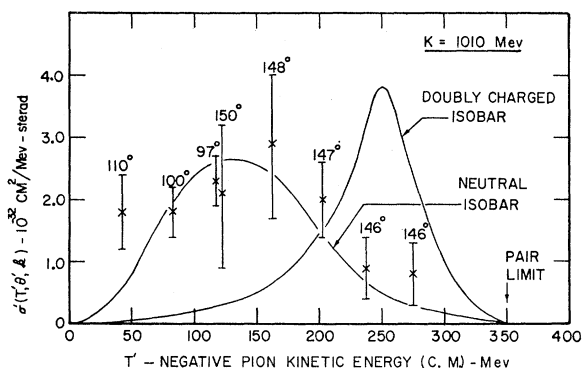


FIG. 8. The c.m. cross section for 1010-Mev photons as a function of the pion kinetic energy (c.m.). The c.m. angle of the negative pion is given for each point.

we can, therefore, assume that our results are a measurement of the pair process. Our data do not, however, show the decrease of the cross section with increasing photon energy above 600 Mev which is reported by Sellen *et al.* In view of the several assumptions we have used to obtain the total cross sections, this disagreement cannot be considered significant.

The cross section for the single production of neutral pions for photon energies from 600 to 1000 Mev has been found<sup>21</sup> to be about 35 microbarns. The cross section for the single production of positive pions in this energy range is about twice this value.<sup>22</sup> It appears that, at these energies, the probabilities of single and double meson emission are roughly equal.

<sup>21</sup> J. I. Vette and W. D. Wales, Bull. Am. Phys. Soc. Ser. II, 6, 320 (1957); R. M. Worlock and A. V. Tollestrup, Bull. Am. Phys. Soc. Ser. II, 6, 320 (1957).

<sup>22</sup> F. P. Dixon and R. L. Walker, Phys. Rev. Letters 1, 142 (1958).



## 4. INTERPRETATION ATTEMPTS

There is, as yet, no theoretical description of the photoproduction of pion pairs at high energies. The Chew-Low theory has been applied by Cutkosky and Zachariasen<sup>5</sup> to calculate the photoproduction of pion pairs near the threshold. These authors have computed the negative pion spectrum, integrated over the pion angle (neglecting all nucleon recoil effects), for several photon energies. The lowest photon energy, 670 Mev, for which we have the pion energy spectrum, corresponds to a center-of-momentum photon energy of 430 Mev. In the static-nucleon theory the maximum pion energy from a 430-Mev photon is 150 Mev, whereas the maximum with a recoiling nucleon is 200 Mev. We compromise by comparing the data to the theoretical curve for 455-Mev photons which allows a maximum pion energy of 175 Mev. The curve labeled C-Z in Fig. 6 is that given by Cutkosky and Zachariasen for  $k=455$  Mev with the cross section divided by  $4\pi$  to obtain the average cross section per unit solid angle.<sup>23</sup> The agreement, both with respect to the magnitude of the cross section and with respect to the dependence

TABLE III. The cross section  $\sigma'(\theta', k)$  for the production in hydrogen of negative pions at c.m. angles from  $95^\circ$  to  $145^\circ$  (per unit solid angle) by photons of energy  $k$ . The total cross section for the emission of negative pions, assuming angular isotropy.

| $k$ (Mev)   | 670 | 830 | 1010 |
|---|-----|-----|------|
| $\sigma'(\theta', k)$ ( $10^{-30}\text{cm}^2/\text{sterad}$ ) | 4.5 | 4.0 | 4.5  |
| $\sigma_t(k)$ ( $10^{-30}\text{cm}^2$ )                       | 56  | 50  | 56   |

on pion energy is certainly satisfactory in view of the meager data and the liberties taken with the theory.

Lacking any theory applicable at the higher energies, we have compared the data to several heuristic models. A simple model is obtained from the assumption that the matrix element for the interaction is independent of the pion energy and angle. The pion energy spectrum is then given by the dependence on pion energy of the density of final states. For the pair process the density of states is proportional to

$$\frac{(E - \omega_+ - \omega_-)\omega_- p_-^3 p_+^2 d\mathbf{p}_+ d\Omega_- d\Omega_+}{(E - \omega_+)p_-^2 + E_-(\mathbf{p}_- \cdot \mathbf{p}_+)}, \quad (14)$$

where  $E$  is the total energy available,  $\omega_+$  and  $\omega_-$  are the pion total energies and  $\mathbf{p}_-$  and  $\mathbf{p}_+$  their momenta, all quantities being taken in the c.m. system. Since we observe only the negative pion, the expression (14) must be integrated over the energies and angles of the positive pion. The integrations<sup>24</sup> have been carried out for photon energies of 650, 800, and 1000 Mev and the results are given in Fig. 9. A comparison with the

<sup>23</sup> The dominant term in the expression given by Cutkosky and Zachariasen corresponds to the negative pion in an  $S$  state.

<sup>24</sup> We are indebted to S. N. Berman for performing these computations.

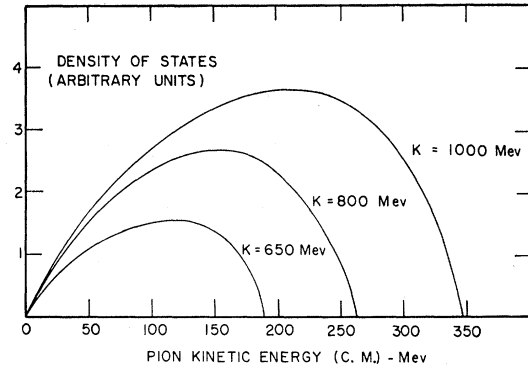


FIG. 9. The negative-pion spectra in the c.m. system given by the three-body density of final states for pair production on protons by photons of energy  $k$ .

experimental data of Figs. 6, 7, and 8 shows that the forms of the spectra are unsatisfactory for all energies.

## Isobar Model

There has been some success in interpreting high-energy pion experiments in terms of an "isobar model" which attempts to take into account the strong interaction between the pion and nucleon in the  $T = \frac{3}{2}$ ,  $J = \frac{3}{2}$  state by considering this state to be sufficiently narrow that it plays the role of a "particle" in the basic interaction. Such a model was first applied by Yuan and Lindenbaum<sup>9</sup> in interpreting the results of pion production in nucleon-nucleon collisions. In later work<sup>11,12</sup> the model was applied to the problem of inelastic pion-nucleon scattering. We have investigated the properties of the isobar model applied to the photoproduction of pion pairs.

Following the earlier workers we assume that in the initial interaction of the photon with the proton two "particles" are produced, a "recoil" pion and an "isobar" of excitation energy  $\omega^*$  (in its coordinate frame). We take that the cross section for the production of an isobar with an excitation energy between  $\omega^*$  and  $\omega^* + d\omega^*$  is

$$d\sigma(E, \omega^*) = A(E)F(\omega^*)d\omega^* \rho(E, \omega^*), \quad (15)$$

where  $E$  is the energy available in the interaction;  $A(E)$  is a factor, taken to be dependent only on  $E$ , which covers our ignorance about the primary interaction;  $F(\omega^*)d\omega^*$  represents an *a priori* weight for the relative probability of forming an isobar of excitation energy  $\omega^*$ ; and  $\rho(E, \omega^*)$  is the density of final states available to the recoil pion and the isobar of mass  $M + \omega^*$ , when the two particles share the available energy  $E$ . Once the dependence on energy of  $F(\omega^*)$  has been assumed, the energy spectrum of the pions can be obtained by straightforward methods. In the present state of ignorance we can take that the isobar is unpolarized and disintegrates isotropically in its rest frame.<sup>25</sup>

<sup>25</sup> The computation of the pion spectra predicted by the isobar model is described in detail by Sternheimer and Lindenbaum in reference 11.

The previous workers have taken  $F(\omega^*)$  to be equal to the observed pion-nucleon scattering cross section in the 3,3 state at an energy corresponding to the excitation  $\omega^*$ . Following a suggestion of Christy<sup>26</sup> we have taken for  $F(\omega^*)$  an expression closely related, but not equal to the cross section. If we write the scattering cross section in the Breit-Wigner form

$$\sigma_{33}(\pi, p) = \frac{8\pi}{q^2} \frac{\frac{1}{4}\Gamma^2}{(\omega^* - \omega_0)^2 + \frac{1}{4}\Gamma^2}, \quad (16)$$

where  $q$  is the pion momentum in the c.m. system of the scattering and  $\hbar = c = \mu = 1$ , it seems most reasonable to take

$$F(\omega^*) = (q^2/\Gamma)\sigma_{33}(\pi, p). \quad (17)$$

The Chew-Low expression for the cross section can be put into the form of Eq. (16) if we take

$$\frac{1}{2}\Gamma = \frac{4}{3}f^2\omega_0q^3/\omega^*, \quad (18)$$

with  $\omega^*$  related to  $q$  by  $\omega^* = (1+q^2)^{1/2} + q^2/2M$ . We have used (16), (17) and (18) to determine  $F(\omega^*)$ , taking  $\omega_0 = 2.1$  and  $f^2 = 0.08$ .

In the photoproduction of pion pairs the isobar model is complicated by the fact that either the negative or positive pion can be bound in the isobar. The reaction can, therefore, proceed through either of two intermediate states:

$$(a) \quad \gamma + p \rightarrow N_{++}^* + \pi^- \rightarrow p + \pi^+ + \pi^-,$$

$$(b) \quad \gamma + p \rightarrow N_0^* + \pi^+ \rightarrow p + \pi^- + \pi^+,$$

where  $N_{++}^*$  and  $N_0^*$  represent two possibilities for the isobar. Reactions (a) and (b) give, of course, completely different forms for the pion spectra. Since the isotopic spin change with the absorption of the photon can be either 0 or 1 (or more), the final state isotopic spin can be either  $\frac{1}{2}$  or  $\frac{3}{2}$ , or a linear combination of the two. In either pure isotopic spin state the reaction should occur predominantly via the "doubly-charged isobar," as in (a) above. For suitable mixtures of the two isotopic spin states, however, the reaction may occur entirely through the doubly-charged isobar or through the "neutral isobar" as in (b) above. Rather than making an assumption about the isotopic spin of the final state, we have computed separately the negative-pion spectra expected from reactions proceeding through either of the two isobars.

The negative-pion spectra predicted by the isobar model are shown by the curves of Figs. 6, 7, and 8 where the vertical scale of the curves has been adjusted arbitrarily to give the best fit to the data. For the two highest energies (830 and 1010 Mev), the spectra from the reaction via the neutral isobar (the negative pion bound to the proton) are in fairly good agreement with the experimental results, whereas the spectra from the doubly-charged isobar are in definite disagreement with

<sup>26</sup> R. F. Christy (private communication).

the data. If one attaches any significance to the model, one would conclude that the reaction must occur through a mixture of isotopic spin states.

At 670 Mev the spectrum from the doubly-charged isobar seems to be in closer agreement with the meager experimental data, although the fit is no better than the Cutkosky-Zachariasen theory which, incidentally, also predicts that the strong interaction in the outgoing state is predominantly between the proton and the positive pion.

One may also remark that the experimental spectra are less sharply peaked than would be given by either isobar model and that the apparent agreement with the neutral isobar model at the higher energies is simply due to the general "smearing" which occurs in this model. Any conclusions in favor of the isobar model will have to wait measurements of pion-pion or pion-proton correlations which will afford a more stringent test of the model.

## 5. POSITIVE PION RESULTS

During the course of the experiment, runs were often made in which positive pions were counted, primarily for checking the operation of the apparatus. These data also give some information about pion pair production. The data for  $60^\circ$  were analyzed in a manner similar to that employed for the negative pions, except that the pion rate was obtained only from the 3-fold coincidence rate, making the now very small electron and background corrections from the corresponding negative-pion data.

The yields per equivalent quantum for positive pions obtained at  $60^\circ$  are shown in Fig. 10. Most of the yield comes, of course, from single-pion production at lower

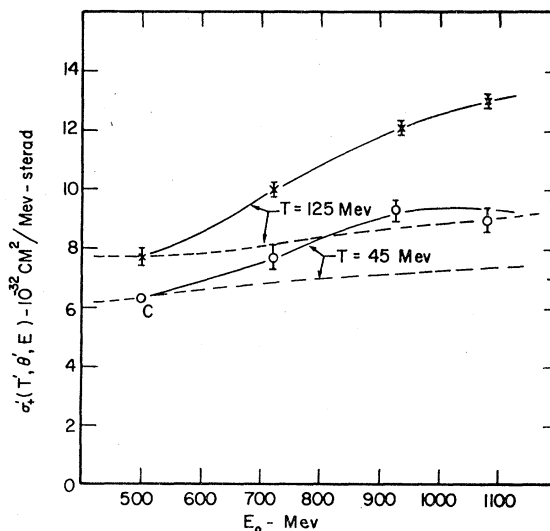


FIG. 10. The positive-pion yields at  $60^\circ$ . The ordinate is the same as for Fig. 3. The dashed curves give the expected dependence on  $E_0$  for pions produced singly. The point marked C was not measured, but was computed from the known cross section for single pion photoproduction.

photon energies:  $k_0=312$  Mev for  $T=50$  Mev, and  $k_0=310$  Mev for  $T=125$  Mev. Also, part of the increase of the yield with increasing  $E_0$  can be attributed to the increase in the single production due to the increase of the number of low-energy photons in the spectrum (see Fig. 5).

A computation of the cross section could be made from the yields as was done for negative pions. It would, however, be of dubious value considering the large errors which would result from the subtraction of two large quantities. Instead, we have computed the expected increase of the yield for single-pion production only. The computed single-pion yields, assumed to be equal to the observed yields at 500 Mev, are shown by the dashed curves in Fig. 10. The difference between

these curves and the experimental curves are to be attributed to pions from the pair process. From a comparison with Fig. 3 we conclude that there are about twice as many positive pions from pairs as there are negative pions. Such a result would be consistent with the assumption that the cross sections for  $(\pi^+, \pi^-)$  pairs and for  $(\pi^+, \pi^0)$  pairs were comparable.

#### ACKNOWLEDGMENTS

We are indebted to the staff of the Synchrotron Laboratory for its cooperation during the course of the experiment, to Professor R. F. Bacher for his interest and support, and to Professor Robert F. Christy, Dr. Jon Matthews, and Dr. F. Zachariasen for several discussions.

### "Anomalous" Scattering of $\mu$ Mesons

SHUJI FUKUI, *Department of Physics, Osaka University, Osaka, Japan*

AND

TAKASHI KITAMURA AND YUZURU WATASE, *Institute of Polytechnics, Osaka City University, Osaka, Japan*

(Received August 21, 1958)

A  $\mu$ -meson scattering experiment in which the mesons are required to traverse a thick block of iron and stop and decay in a thin layer of carbon, is reported. Any uncertainty in the identity of the scattered particle has thus been eliminated, and further, the momentum of the particles is well defined. The observed angular distribution of the scattered  $\mu$  mesons in the momentum range  $(1_{-0.2}^{+0.15})$  Bev/c has been found to be in good agreement with the distribution predicted from the Coulomb scattering theory for extended nuclei obtained by Cooper and Rainwater. There is thus no indication from the present experiment for any anomalous scattering of  $\mu$  mesons near 1 Bev/c momentum.

The angular distribution of scattering of those particles which traversed the iron absorber but did not necessarily stop and decay in the carbon layer was not in good agreement with the Cooper and Rainwater theory, there being more than the expected number of particles scattered through large angles. It is shown, however, that the predicted scattering distribution, at large angles (assuming no anomalous contribution) arises almost entirely from the scattering of particles in the 1-2 Bev/c region, and therefore is very sensitive to the assumed intensity in this region. It is concluded that the results from this part of the experiment cannot be accepted as evidence favoring the existence of anomalous scattering.

The experimental results of other authors on the scattering of energetic  $\mu$  mesons are summarized and discussed. It is concluded that the evidence for anomalous interactions is not strong.

#### I. INTRODUCTION

THE  $\mu$  meson, in its interaction with matter, is believed to behave as a heavy ( $207 m_e$ ) electron. That is, the  $\mu$  meson evidently interacts mainly through its electromagnetic field, but in addition may interact with the emission and absorption of neutrinos.<sup>1</sup> There are a number of experiments which support this view. Walker<sup>2</sup> has observed the knock-on electrons produced by  $\mu$  mesons of energy larger than 1.5 Bev. The electrons had an energy distribution consistent with that to be

expected from electromagnetic interactions alone. Barrett *et al.*<sup>3</sup> have observed parallel pairs of  $\mu$  mesons deep underground, and have concluded that these parallel pairs would not be expected if there were other than purely electromagnetic interactions. Fitch and Rainwater<sup>4</sup> have investigated the level structure of  $\mu$ -mesonic atoms and their results are consistent with the assumption that the  $\mu$  meson interacts only electromagnetically with nuclei. Masek and Panofsky, and Masek, Lazarus, and Panofsky<sup>5</sup> have observed the

<sup>1</sup> For example, R. E. Marshak, *Meson Physics* (McGraw-Hill Book Company, Inc., New York, 1952), Chap. 6; B. Rossi, *High-Energy Particles* (Prentice-Hall, Inc., Englewood Cliffs, New Jersey, 1952), Chap. 4.

<sup>2</sup> W. D. Walker, Phys. Rev. **90**, 234 (1953).

<sup>3</sup> Barrett, Bollinger, Cocconi, Eisenberg, and Greisen, Revs. Modern Phys. **24**, 133 (1952).

<sup>4</sup> V. L. Fitch and J. Rainwater, Phys. Rev. **92**, 789 (1953).

<sup>5</sup> G. E. Masek and W. K. H. Panofsky, Phys. Rev. **101**, 1094 (1956); Masek, Lazarus, and Panofsky, Phys. Rev. **103**, 374 (1956).